CHAPTER III

RESEARCH METHODOLOGY

This section outlines the research methodology, including simulations using the UrQMD program and the implementation of light nuclei formation within the framework, followed by details on data analysis. In addition, the UrQMD simulation model is introduced.

3.1 The UrQMD transport model

The Ultrarelativistic Quantum Molecular Dynamics model (UrQMD) is a microscopic simulation model employed for (ultra)relativistic heavy-ion collisions across an energy spectrum spanning from Bevalac and SIS up to AGS, SPS, and RHIC. Its primary objectives encompass achieving a deeper comprehension of various aspects, including the formation and characteristics of dense hadronic matter at elevated temperatures, properties of nuclear matter and resonance states, the generation of mesonic matter and antimatter, as well as the production and transport of rare particles within hadronic matter. Additionally, UrQMD is instrumental in studying the creation, modification, and annihilation of strangeness in matter, along with the emission of electromagnetic probes (Bass et al., 1998; Bleicher et al., 1999). For our simulation of heavy-ion collisions, we utilize the UrQMD model, which incorporates a coalescence model for the dynamic formation of nuclei from protons and neutrons with identical momenta and positions. In our simulation, the program was in version 3.4 and we also configured the model to operate in coalescence mode, considering projectile masses corresponding to a mass of 197 (the mass of Au, gold). We conducted a simulation of Au+Au collisions from t =1 fm/c until 60 fm/c across a range of beam energies from 2.0 AGeV to 3.0 AGeV with 1.0 AGeV increment.

This model incorporates a density-dependent Equation of State (EoS) by introducing an effective density-dependent potential into the non-relativistic Quantum Molecular Dynamics (QMD) (Aichelin et al., 1986; Hartnack et al., 1989; Stoecker et al., 1986) equations of motions,

$$\dot{\mathbf{r}}_i = \frac{\partial H}{\partial p_i}, \qquad \dot{p}_i = -\frac{\partial H}{\partial r_i}. \tag{20}$$

In this context, the total Hamiltonian of the system, denoted as H, encompasses both the kinetic energy and the overall potential energy, which can be expressed as $V = \sum_i V_i \equiv \sum_i V\big(n_B(r_i)\big)$. The equations of motion are then solved, taking into account that the potential energy V is straightforwardly related to the pressure (Steinheimer, Motornenko, et al., 2022).

$$P(n_B) = P_{\text{id}}(n_B) + \int_0^{n_B} n' \frac{\partial U(n')}{\partial n'} dn' \tag{21}$$

Here, $P_{\text{id}}(n_B)$ represents the pressure of an ideal Fermi gas of baryons, and $U(n_B) = \frac{\partial\big(n_B \cdot V(n_B)\big)}{\partial n_B}$ denotes the single particle potential.

3.2 Implementation of a phase transition in UrQMD

Implementing a phase transition into the CMF model, involves a straightforward modification (Savchuk et al., 2023). To introduce an additional meta-stable state within the mean field energy per baryon at high densities, apart from the existing bound state resulting from the nuclear liquid-gas transition, an adjustment is made to the original chiral mean field (CMF) potential. This adjustment consists of truncating the potential at a density of $2.6\, n_0$. Beyond this density threshold, the potential $V(n_B)$ is then shifted by an amount $\Delta n_B = 2.6\, n_0$.

The selection of the n_{cut} value is influenced by two key considerations:

1. To ensure the attainability of the transition through heavy ion collision experiments, it is essential to restrict the density range to $n_B^{cut} < 4 - 5 n_0$ (Omana Kuttan et al., 2022).
2. The chosen density surpasses the threshold of $2 n_0$ to prevent any inconsistencies with the existing constraints derived from heavy ion collisions and observations in astrophysical contexts (Huth et al., 2022).

The mean field energy within the range of $n_B^{cut} < n_B < n_B^{cut} + \Delta n_B$ is interpolated using a third-order polynomial. This interpolation is carried out to establish a secondary minimum in the energy per particle, denoted as $V(n_B)$. This approach guarantees the continuity of both the energy function and its derivative.

Figure 3.1 represents the evolution in the pressure and net baryon density at $T = 0$ compared to the normal CMF EoS and the implemented phase transition EoS. The red shading area corresponds to the region of mechanical instabilities, where the system created after a collision rapidly separated into the two coexisting phases. This

mechanism is known as spinodal decomposition. One can observe a non-monotonic behavior in the blue line, which reflects the nature of the phase transition.

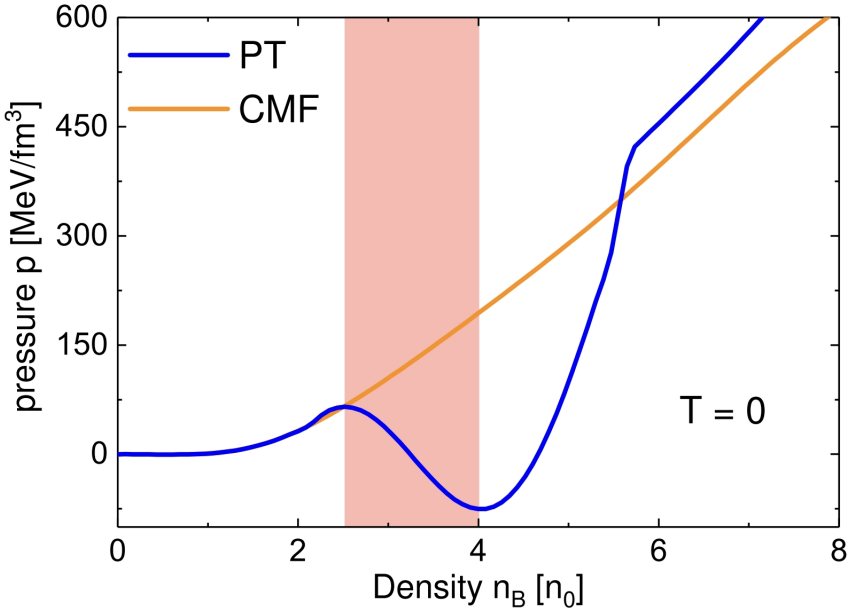

Figure 3.1 Time evolution in pressure and baryon density at $T = 0$ between the two scenarios: the CMF EoS with no phase transition (orange line) and the phase transition EoS (blue line). The red shading area refers to a region where the pressure gradient is negative: the spinodal region (Savchuk et al., 2023).

3.3 Light nuclei production in UrQMD

3.3.1 Deuteron production

The implementation of phase-space coalescence done in UrQMD for deuterons in the following way (Sombun et al., 2019):

1. Throughout the system's time evolution, we track the trajectories of protons and neutrons until the specific spacetime coordinates where their final interactions occur.
2. In the case of each proton-neutron pair, the momentum and position of both the proton and neutron are adjusted to match the 2-particle rest frame of this pair.
3. The particle that has decoupled at an earlier time is subsequently advanced to the later time of the other particle in the system.
4. The relative momenta $\Delta p = |\overrightarrow{p_1} - \overrightarrow{p_2}|$ and the relative distances $\Delta r = |\overrightarrow{x_1} - \overrightarrow{x_2}|$ are computed for the proton-neutron (p-n) pair in the 2-particle rest frame when their times are equal. The yield of deuteron candidates is determined by satisfying the conditions

$\Delta p < \Delta p_{max}$ and $\Delta r < \Delta r_{max}$. In this particular case, we have set the parameters to $\Delta p_{max} = 0.285$ GeV/c and $\Delta r_{max} = 3.575$ fm.

3.3.2 Triton and helium-3 production

For tritons and helium-3, we use (Hillmann et al., 2022):

1. We examine the two-particle rest frame for every possible two-nucleon pair. If the relative distance between them ($\Delta r = |\overrightarrow{r}_{n_1} - \overrightarrow{r}_{n_2}|$) is less than $\Delta r_{max,nn} = 3.575$ fm, and the momentum distance $\Delta p = |\overrightarrow{p}_{n_1} - \overrightarrow{p}_{n_2}|$ is less than $\Delta p_{max,nn} = 0.285$ GeV/c, it suggests the potential formation of a two-nucleon state. In this case, the combined momenta are represented as $\overrightarrow{p}_{nn} = \overrightarrow{p}_{n_1} + \overrightarrow{p}_{n_2}$, and the position is given by $\overrightarrow{r}_{nn} = \frac{1}{2}(\overrightarrow{r}_{n_1} + \overrightarrow{r}_{n_2})$. These parameters, $\Delta r_{max,nn}$ and $\Delta r_{max,nn}$, align with those previously determined for the deuteron. The subscripts here denote the momentum and position with a given nucleon state.

2. In this step, we transition into the local rest frame of this two-nucleon state and any possible third nucleon. Under the condition that their relative separation ($\Delta r = |\overrightarrow{r}_{nn} - \overrightarrow{r}_{n_3}| < \Delta r_{max,nnn}$) and momentum difference ($\Delta p = |\overrightarrow{p}_{nn} - \overrightarrow{p}_{n_3}| < \Delta p_{max,nnn}$), a triton with a charge of 1 or a helium-3 with a charge of 2 is generated with a likelihood of $\frac{1}{12} \cdot \frac{1}{3!}$. Here, the initial factor corresponds to the spin-isospin coupling, and the subsequent factor accommodates the diverse permutations that produce the same nnn-state. The momentum of the resulting three-nucleon state is then computed as $\overrightarrow{p}_{nnn} = \overrightarrow{p}_{nn} + \overrightarrow{p}_{n_3}$, and the position is determined as $\overrightarrow{r}_{nnn} = \frac{1}{3}(\overrightarrow{r}_{n_1} + \overrightarrow{r}_{n_2} + \overrightarrow{r}_{n_3})$.

3. In the absence of a third particle and in cases where the charge equals 1, the creation of a deuteron is carried out with a probability of $\frac{3}{8} \cdot \frac{1}{2!}$. The initial factor in this probability accounts for the spin-isospin coupling, while the subsequent factor accommodates the various combinations that lead to the same nn-state. This particular treatment for deuterons mirrors the methodology previously described in the citation (Sombun et al., 2019), with the additional factor of $\frac{1}{2!}$ introduced to address the issue of combinatorial double counting in the numerical procedure.

3.3.3 Helium-4 production

The procedures on this nuclear cluster follow the previous steps as mentioned in the previous section on the triton and helium-3 production. However, the coalescence parameter Δr_{ij} and Δp_{ij} were fitted separately to the measurements from the E864 experiment (Armstrong et al., 2000).

In order to provide an agreement between results from the UrQMD simulation model with additional implementations on how nuclear clusters were produced and experimental data, results taken from various experiments as well as the thermal model fit, were included in the comparison. Figure 3.2 displays the beam-energy dependence of the ratios for both d/p and $\bar{d}/\bar{p}$ along with corresponding experimental data. It is obvious to see that the ratios $\frac{d}{p}$ and $\frac{\bar{d}}{\bar{p}}$ are consistently agreed with both the thermal model fit and the experimental data. This agreement supports the validity of the simulation model with the implemented modifications on the nuclear cluster production in coalescence approach.

3.4 UrQMD simulation

For our simulation of heavy-ion collisions, we utilize the UrQMD model, which incorporates a coalescence model for the dynamic formation of nuclei from protons and neutrons with identical momenta and positions. In our simulation, the program was in version 3.4 and we also configured the model to operate in coalescence mode, considering projectile masses corresponding to a mass of 197 (the mass of Au, gold). We conducted a simulation of Au+Au collisions from $t = 1$ fm/c until 40 fm/c across a range of beam energies from $E_{\text{lab}} = 2.0$ AGeV to 3.0 AGeV.

3.5 Data analysis

After the simulation, the outputs of interest are stored in files with the extension ".f13". In contrast to the usual UrQMD output which gives particle vectors only at the freeze-out, we store the complete time evolution of the collisions. On these files, we perform our data analysis by text processing Python code via Jupyter Notebook to extract particle vectors including particle type (itype), coordinate (x,y,z), electric charge. Here the light nuclei: free proton (p), deuteron (d), triton (t), helium-3 (^3He), and helium-4 (^4He) are our particles of interest. After that we count only particles whose coordinates lie within a spatial volume defined as a sphere with 2 fm radius located at origin (0,0,0) and average their multiplicities over the whole set of events for each time step. Then we can plot the time evolution in light nuclei production for given beam energies. We repeat this procedure for cuts in momentum space rather than position space as it is done by experiments.

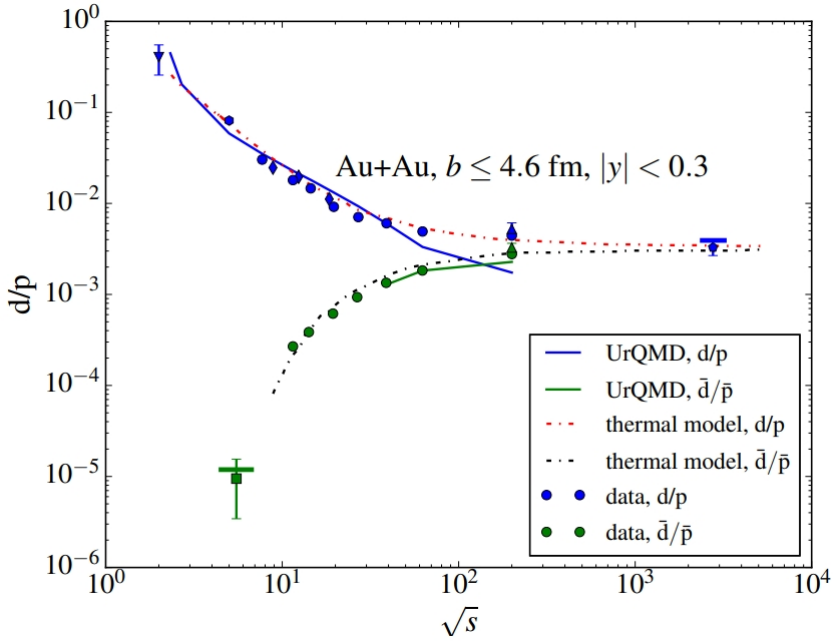

Figure 3.2 Beam-energy dependence of the deuteron to proton ratio from the UrQMD simulation (solid lines), thermal model fit (dotted lines). The symbols of different styles denote the experimental data from the corresponding collaborations: SIS (triangle down), E802 (hexagon), PHENIX (triangles up), NA49 (blue diamonds), STAR (circles), ALICE (pentagon), E814 (square). The blue horizontal line represents the UrQMD+hydro result on the d/p ratio at 2.76 TeV and the green horizontal line represents the UrQMD result of the $\frac{\bar{d}}{\bar{p}}$ ratio in Si+Au collisions at $E_{\text{lab}} = 14.6\ A$GeV (Sombun et al., 2019).

3.5.1 Propagation of the light nuclei in coordinate space

As far as we have tracked the position in particle time steps, we need to obtain their positions in the coordinate space (within a spatial volume). The position as a function of time can be expressed as a vector function:

$$\overrightarrow{r}\ (t) = \overrightarrow{r}\ (t_{fr}) + \overrightarrow{v}\ (t_{fr})\Delta t \tag{22}$$

where $\overrightarrow{r}\ (t)$ is the position of the particle at its proper time t, t_{fr} is freeze-out time with $\Delta t = t - t_{fr}$ and $\overrightarrow{v} = \frac{\overrightarrow{p}}{E}$ is the particle's relativistic velocity.

Once the particle positions are obtained, we then proceed to count only the particles that locate within the volume of the sphere i.e., $|\overrightarrow{r}| < 2.0$ fm and continue to perform calculation on their fluctuations.

The next chapter will be presenting the results, where the calculated fluctuations are analyzed and interpreted.